Revealing lymphoma growth and the efficacy of immune cell therapies using in vivo bioluminescence imaging

Matthias Edinger, Yu-An Cao, Michael R. Verneris, Michael H. Bachmann, Christopher H. Contag, and Robert S. Negrin

Cancer therapeutics have achieved success in the treatment of a variety of malignancies, however, relapse of disease from small numbers of persistent tumor cells remains a major obstacle. Advancement of treatment regimens that effectively control minimal residual disease and prevent relapse would be greatly accelerated if sensitive and noninvasive assays were used to quantitatively assess tumor burden in animal models of minimal residual disease that are predictive of the human response. In vivo bioluminescence imaging (BLI) is an assay for the detection of small numbers of cells noninvasively and enables the quantification of tumor growth within internal organs. Fusion genes that encode bioluminescent and fluorescent reporter proteins effectively couple the powerful in vivo capabilities of BLI with the subset-discriminating capabilities of fluorescence-activated cell sorting. We labeled 2 murine lymphoma cell lines with dual function reporter genes and monitored radiation and chemotherapy as well as immune-based strategies that employ the tumorcidal activity of ex vivo–expanded $CD8^+$ natural killer (NK)–T cells. Using BLI we were able to visualize the entire course of malignant disease including engraftment, expansion, metastasis, response to therapy, and unique patterns of relapse. We also labeled the effector NK-T cells and monitored their homing to the sites of tumor growth followed by tumor eradication. These studies reveal the efficacy of immune cell therapies and the tempo of NK-T cell trafficking in vivo. The complex cellular processes in bone marrow transplantation and antitumor immunotherapy, previously inaccessible to investigation, can now be revealed in real time in living animals. (Blood. 2003;101: 640-648)

Introduction

Radiation and chemotherapy have proven to be effective treatments for patients with a variety of malignant disorders, however, relapse from minimal residual disease states remains a significant challenge to effective treatment. Following high-dose chemotherapy and autologous or allogeneic bone marrow transplantation (BMT), nearly all patients achieve what appears to be a complete remission where disease is no longer detectable with available imaging techniques or biochemical or molecular assays. However, a significant percentage of these patients ultimately relapse, indicating that malignant cells were still present, yet undetectable. The reduced relapse rate following allogeneic, as compared to autologous, BMT provides compelling evidence that minimal residual disease can be controlled by immunological mechanisms.[1-3] The development of adoptive cellular therapies that selectively enhance graft-versus-tumor (GVT) effects after allogeneic BMT may therefore significantly improve treatment outcomes.

Animal models that can be readily evaluated and that are predictive of the human response are critically important for the advancement of more effective therapies and for enhancing our understanding of cancer cell biology and immune surveillance. However, the study of animal models has been limited by the difficulty of accurately assessing disease burden and response to therapy, especially in minimal disease. External tumor measurements, for example, with calipers or by gross inspection, are limited to diseases at accessible sites. Biochemical and molecular assays typically require humane animal killing and are complicated by the possibility of sampling artifacts. In an effort to overcome some of these limitations, a variety of techniques have been developed to trace cells in vivo, including labeling cells with fluorescent dyes, bromodeoxyuridine, and radioisotopes. These techniques can be hampered by cytotoxic side effects of the labeling procedures and can be limited due to dilution, and, finally, loss of the marker over time as a result of cell division.[4] The latter problem has been, in part, overcome by recent advances in viral transduction methods that allow the transfer and stable integration of reporter genes such as green fluorescent protein (GFP) into the genomic DNA of cells. Furthermore, the development of GFP-expressing transgenic animals offers the opportunity for near-limitless sources of labeled cell populations with sufficient stability of the reporter gene.[5] Such optical markers permitted the evaluation of labeled cells by fluorescence microscopy and flow cytometry. However, both of these methods require isolation of the cells for analysis and, therefore, humane killing of the study subjects. This eliminates the possibility of gathering important spatiotemporal

From the Division of Bone Marrow Transplantation, Department of Medicine; and Department of Pediatrics; Stanford University School of Medicine; Stanford, CA.

Submitted August 9, 2002; accepted August 15, 2002. Prepublished online as *Blood* First Edition Paper, September 26, 2002; DOI 10.1182/blood-2002-06-1751.

Supported by the Dr Mildred Scheel Cancer Research Foundation (M.E.) and National Institutes of Health grants P01 CA49605 (R.S.N.), R33 CA88303 (C.H.C.), R24 CA92862 (C.H.C.), P20 CA86312 (C.H.C.), R01 CA80006 (R.S.N.), and KO8 HLO4505-01 (M.R.V.).

C.H.C. is a scientific founder and consultant of Xenogen Corp.

Reprints: Robert S. Negrin, Center for Clinical Sciences Research Building, Rm 2205, 269 W Campus Dr, Stanford, CA 94305-5290; e-mail: negrs@stanford.edu.

The publication costs of this article were defrayed in part by page charge payment. Therefore, and solely to indicate this fact, this article is hereby marked "advertisement" in accordance with 18 U.S.C. section 1734.

information about cellular trafficking patterns, the dynamics of cell proliferation, and the kinetics of cell death within a given animal. This information, however, is essential if one wishes to reveal the cellular events leading to complex biologic processes such as tumor recognition and eradication by immune cells in vivo.

In vivo bioluminescence imaging (BLI) has enabled the study of tumor cell growth and offers sensitivity as well as a broad dynamic range of quantification. In the presence of oxygen and magnesium, the reporter gene luciferase produces visible light from a small molecule substrate, luciferin, in the presence of oxygen and adenosine triphosphate.[6,7] Since visible light penetrates tissues at low levels, cells expressing this enzyme can be followed in living animals by external detection of the emitted light using low-light imaging systems.[8-11]

To extend this approach to syngeneic animal models and to further refine this strategy, we have used dual function reporter genes that code for a fluorescent marker (either green or yellow fluorescent protein, GFP or YFP) for ex vivo cell sorting and a bioluminescent marker for in vivo imaging. We used these reporter genes to label the BALB/c-derived BCL_1 and A20 B-cell lymphomas, and we monitored disease growth and metastasis following intravenous injection into syngeneic recipients. The initial trafficking of the malignant cells through the body, as well as organ-specific homing and orthotopic expansion over time, was readily visualized and quantitated. Furthermore, the response of established BCL_1 and A20 tumors to immune cell therapies and more conventional therapies such as radiotherapy and chemotherapy was monitored in real time and under physiological conditions. In vitro–activated and –expanded effector T cells that have both functional and phenotypic properties of natural killer (NK) cells, termed cytokine-induced killer (CIK) cells, were used in this study. By tagging the effector cells, we were able to noninvasively monitor effector cell trafficking patterns relative to tumor eradication during immunotherapy. The ability to monitor the entire disease course over time revealed tumor-specific escape strategies, as signals from the lymphoma cells could be detected in the central nervous system following high-dose irradiation.

Materials and methods

Animals

Female C57BL/6 (H-2K^b) and BALB/c (H-2K^d) mice were obtained from the breeding facility of the Department of Comparative Medicine, Stanford University, CA. All mice were used between 6 and 12 weeks of age. Care of all experimental animals was in accordance with institutional guidelines on approved protocols.

Retroviral vectors

The pGC-*gfp/luc* vector and the transfection procedure of Phoenix-E producer cells have been described previously.[12] The pGC-*gfp/luc* construct was a kind gift of C. G. Fathman, Stanford University. The retroviral backbone MND-X-SN was described previously[13] and was a kind gift of D. B. Kohn, University of Southern California, Los Angeles, CA. The yellow-green luciferase was amplified by polymerase chain reaction from pGL3-Basic (Promega, Madison, WI) using the 5′ primer ATGAATTCA-AGCTTATGGAAGACGCCAAAAACATAAAGAAAGGCCCGGCGCCA-TTCT-ATC and the 3′ primer CTGATCCTTAGGTACCCCTCCACCCAG-CCCGCCTGAACCTCCCACGGC-GATCTTTCCGCCCTTCTTGGCCTT-TATGAGGATC. The amplified luciferase cDNA consisting of the entire luciferase coding sequences without a stop codon and a linker of 27 nucleotides encoding for 9 amino acids was inserted into the *Hin*dIII and *Kpn*I sites of the pEYFP-N1 vector (Clontech, Palo Alto, CA) in-frame with a cDNA encoding an enhanced yellow-green variant of the GFP. The full-length linker between luciferase and EYFP is 60 nucleotides (GGAG-GTTCAGGCGGGCTG-GGTGGAGGGGTACCGCGGGCCCGGGATC-CACCGGTCGCCACC), including 33 from the 5′ of the EYFP-N1. The resulting luciferase-EYFP fusion was then cloned into the *Hin*dIII and *Not*I sites of the pcDNA3.1 (+) vector (Invitrogen, Carlsbad, CA). A *Pme*I to *Xho*I fragment of *luc*-EYFP from pcDNA3.1/*luc*-EYFP was then inserted in between the *Hpa*I and *Xho*I sites of the MND-X-SN vector, and the final construct was named MND-*luc/yfp/neo.*

Transduction of lymphoma cells

BCL_1 lymphoma cells were passaged through BALB/c mice, isolated from spleens of tumor-bearing animals, and cryopreserved. Thawed cells were resuspended in RPMI 1640 (Gibco BRL, Gaithersburg, MD) containing 10% fetal calf serum, 2 mM L-glutamine, 100 U/mL penicillin, 100 μg/mL streptomycin, and 50 μM 2-mercaptoethanol (all from Sigma, St Louis, MO) (cRPMI), and stimulated with 5 μg/mL lipopolysaccharide (LPS) (Sigma) for 24 hours. Supernatant was removed and cells were cultured in recombinant retroviral supernatant (pGC-*gfp/luc*) supplemented with 4 μg/mL polybrene (Sigma) and 5 μg/mL LPS. Cells were analyzed and sorted for GFP expression 48 hours after transduction, and 7×10^3 GFP$^+$ cells were injected intravenously into 6- to 9-week-old BALB/c mice. Tumor cells were re-isolated from animals with advanced disease, and GFP$^+$ cells were passaged through 4 generations of BALB/c mice to guarantee stable and homogeneous GFP and luciferase expression, and then through severe combined immunodeficient (SCID) mice to avoid lymphocyte contamination at the time of cryopreservation. This line is referred to as BCLf1-*gfp/luc*.

The A20 cell line (ATCC, Rockville, MD) was stimulated with 5 μg/mL LPS in cRPMI and retrovirally transduced as described for the BCL_1 cell line with the MND-*luc/yfp/neo* plasmid. Transduced cells were cultured in 1 mg/mL G418 (Gibco BRL), outgrowing cells were single-cell cloned, and a high-expressing clone was further expanded (A20-*luc/yfp/neo*) and cryopreserved.

Isolation and transduction of lymphocytes

Lymphocytes from liver were isolated as described by Eberl and MacDonald[14] and from spleens as described previously.[15] For the generation of transduced CIK cells, BALB/c (H-2^d) splenocytes were stimulated in cRPMI (3×10^6/mL) with 1000 U/mL rmIFN-γ (R&D Systems, Minneapolis, MN) for 24 hours, transferred to an anti-CD3 (145-2C11, BD Pharmingen, San Diego, CA) antibody–coated tissue-culture flask, and stimulated with 300 U/mL rhIL-2 (Chiron, San Francisco, CA). After 36 hours of IL-2 and anti-CD3 stimulation, 5×10^6 cells were resuspended in 2.5 mL retroviral supernatant (pGC-*gfp/luc*) supplemented with 8 μg/mL protamine sulfate (Sigma) and 300 U/mL rhIL-2, placed in one well of a 6-well plate, and centrifuged for 20 minutes at 2300 rpm and 32°C. Cells were cultured in 32°C, 5% CO_2 for 8 hours, then transferred to 37°C, 5% CO_2. At 24 hours after transduction, 4 mL cRPMI and rhIL-2 were added, and 48 hours after transduction, cells were sorted by flow cytometry for GFP$^+$ cells. Cells were expanded for 14-21 days in cRPMI containing 300 U/mL rh IL-2 and analyzed by flow cytometry prior to injection. Cells usually were 20%-30% GFP$^+$ and showed the previously described phenotype.[15]

Bone marrow transplantation of tumor-bearing hosts

Female 8- to 12-week-old BALB/c mice received 2×10^3 BCL_1-*gfp/luc* cells intravenously and were monitored for tumor growth by bioluminescence imaging 7 days after tumor inoculation. For bone marrow transplantation, tumor-bearing hosts were given total body irradiation (8 Gy) from a 200 Kv x-ray source and injected with donor cells via the tail vein within 24 hours. All mice received 5×10^6 bone marrow (BM) cells for reconstitution with or without T cells or CIK cells as indicated in the text and figures. Mice were kept on antibiotic water (sulfomethoxazole/trimethoprim, Schein Pharmaceutical, Port Washington, NY) for the first 28 days. Survival and

appearance of mice were monitored daily, and body weight was measured weekly.

In vivo imaging

Mice were anaesthetized with ketamine (100 mg/kg intraperitoneally) (Fort Dodge Animal Health, Fort Dodge, IA) and xylazine (10 mg/kg intraperitoneally) (Butler, Columbus, OH), and an aqueous solution of luciferin (150 mg/kg intraperitoneally) (Xenogen, Alameda, CA) was injected 5 minutes prior to imaging. Animals were placed into the light-tight chamber of the CCD camera system (IVIS, Xenogen), and a grayscale body surface reference image (digital photograph) was taken under weak illumination.[16] After switching off the light source, photons emitted from luciferase-expressing cells within the animal body and transmitted through the tissue were quantified over a defined period of time ranging up to 5 minutes using the software program "Living Image" (Xenogen) as an overlay on Igor (Wavemetrics, Seattle, WA). For anatomical localization, a pseudocolor image representing light intensity (blue, least intense; red, most intense) was generated in "Living Image" and superimposed over the grayscale reference image. Annotations were added using another graphics software package (Canvas 5.0, Deneba, Miami, FL). Animals examined for quantification of BCL_1-*gfp/luc* tumor growth were imaged from a left lateral position, and animals bearing A20-*luc/yfp* tumors were imaged from the ventral position.

Antibodies and flow cytometric analysis

The following reagents were used for flow cytometric analysis (FACS): unconjugated anti-CD16/32$^{2.4G2}$, phycoerythrin (PE)–anti-CD19^{1D3}, PE–anti-CD45$^{30\text{-}F11}$, and PE–anti-IgM (R6-60.2). Antibodies were purchased from BD Pharmingen. All staining was performed in phosphate-buffered saline/1% calf serum in the presence of purified anti-CD16/32 at saturation to block unspecific staining via FcRII/III. Propidium iodide was added prior to analysis to exclude dead cells. Flow cytometric analyses were performed on FACScan or a modified dual-laser FACS Vantage (Becton Dickinson, San Jose, CA), and data were analyzed using FlowJo software (Tree Star, San Carlos, CA). At least 10 000 cells were analyzed. Cells analyzed for GFP or YFP expression were examined in the fluorescein isothiocyanate (FL1) channel.

Statistical methods

Percent signal reduction following chemotherapy or irradiation therapy was calculated according to the formula: % signal reduction = 100 − [signal intensity day 4 after treatment − background signal intensity] × 100/[pretreatment signal intensity − background signal intensity]. Background signal was determined by imaging 10 sex- and age-matched BALB/c animals that did not receive luciferase-transduced cells. Data are reported as mean and range. Differences in survival of groups of hosts given BM transplants were analyzed using the log-rank test.

Results

Spatiotemporal tracking of BCL_1-*gfp/luc* and A20-*luc/yfp* B-cell lymphoma cells in vivo

The BALB/c-derived B-cell lymphoma cell line BCL_1 was chosen as one of the first model tumors because of its known homing pattern to liver and spleen in recipient BALB/c animals.[17,18] Since BCL_1 cells cannot be maintained long-term in culture, a retroviral transduction system was used for the delivery of a *gfp/luc* fusion gene. Cells were transduced 24 hours after thawing and then sorted by FACS for GFP expression. GFP^+ BCL_1 cells were passaged 4 times through syngeneic recipients and finally through BALB/c SCID mice before cryopreservation. The resulting BCL_1-*gfp/luc* tumor cells showed a homogenous expression of GFP (Figure 1A). The time course of engraftment and organ-specific expansion of 7×10^3 BCL_1-*gfp/luc* cells after intravenous injection into BALB/c animals is shown in Figure 1B. All recipients showed tumor engraftment. Shortly after injection, a bioluminescent signal could be detected over the lungs. Repetitive imaging of individual animals on the following days demonstrated tumor cell homing to the spleen by day 5, followed by a logarithmic growth phase in spleen and liver, as quantitated at weekly intervals by measuring the amount of light emitted from the body of the animals over a 5-minute integration time (Figure 1C). Despite this progressive tumor growth that was readily demonstrable by BLI, the animals appeared normal until several weeks later, when disease manifestation characterized by ascites and wasting became evident. At that stage, BLI revealed massive hepatosplenomegaly with metastasis to the lungs (Figure 1B) as well as the BM and a leukemic distribution of tumor cells (not visible in Figure 1B because sensitivity of detection was adjusted for optimal display of organ infiltration). At the same time, tumor cells within the spleen also could be visualized by fluorescence microscopy, revealing diffuse infiltration and effacement of the splenic architecture (data not shown).

Similar studies were performed in a second tumor model after retroviral transduction of the BALB/c-derived A20 lymphoma/leukemia cell line with a vector delivering a *luc/yfp* fusion construct. Transduced A20-*luc/yfp* cells (2×10^4) were injected intravenously into sublethally (4 Gy) irradiated BALB/c recipient mice. Within 7 days, homing of the tumor cells to the bone marrow cavity was readily apparent with signal over the bilateral humeri and femurs, as well as sternum and vertebrae (Figure 2A). Again, tumor growth in the bone marrow cavity could be quantitatively assessed by serial determination of the amount of light emitted from individual animals, which revealed a growth lag phase of 5 to 7 days, followed by a logarithmic growth period until day 21 (Figure 2B). FACS analysis on day 21 confirmed the bone marrow infiltration and showed that more than 60% of the isolated BM cells were indeed $CD19^+$ YFP^+ tumor cells (Figure 2C).

To address the question as to what extent light emission quantified by BLI accurately reflects the total tumor burden of an animal, a series of 15 BCL_1-*gfp/luc* tumor-bearing animals at various stages of disease were first evaluated by BLI, then humanely killed, and the percentages of GFP^+ cells in liver and spleen were determined by FACS analysis. Because BCL_1 tumor cells are found almost exclusively in these 2 organs until late in the disease course, the total number of splenocytes and hepatic lymphocytes was multiplied by the percentage of GFP^+ cells to approximate the total number of BCL_1 tumor cells. A linear correlation between the number of tumor cells as determined by FACS analysis and the BLI signal intensity was obtained over at least 4 logs of tumor burden ($r = 0.989$; Figure 3A). The lowest level of GFP^+ tumor cells detectable by FACS in the spleen was 2.3×10^4. BLI, however, was significantly more sensitive, and we could reliably detect labeled tumor cells within the spleen even before they were detectable by FACS. Representative FACS patterns of liver and spleen from animals with either high (top panels) or low tumor burden (bottom panels) are shown in Figure 3B.

Response to chemotherapy and radiation therapy revealed in vivo in an orthotopic tumor model

To evaluate the response of an established B-cell lymphoma to therapeutic interventions in vivo and in real time, BALB/c recipients were injected with 2×10^3 BCL_1-*gfp/luc* tumor cells, and their orthotopic tumor growth was assessed by BLI after 14 days. As expected, animals within a control group that received no further treatment showed a continuous increase in their tumor signal (Figure 4A). In contrast, treatment of a second group of

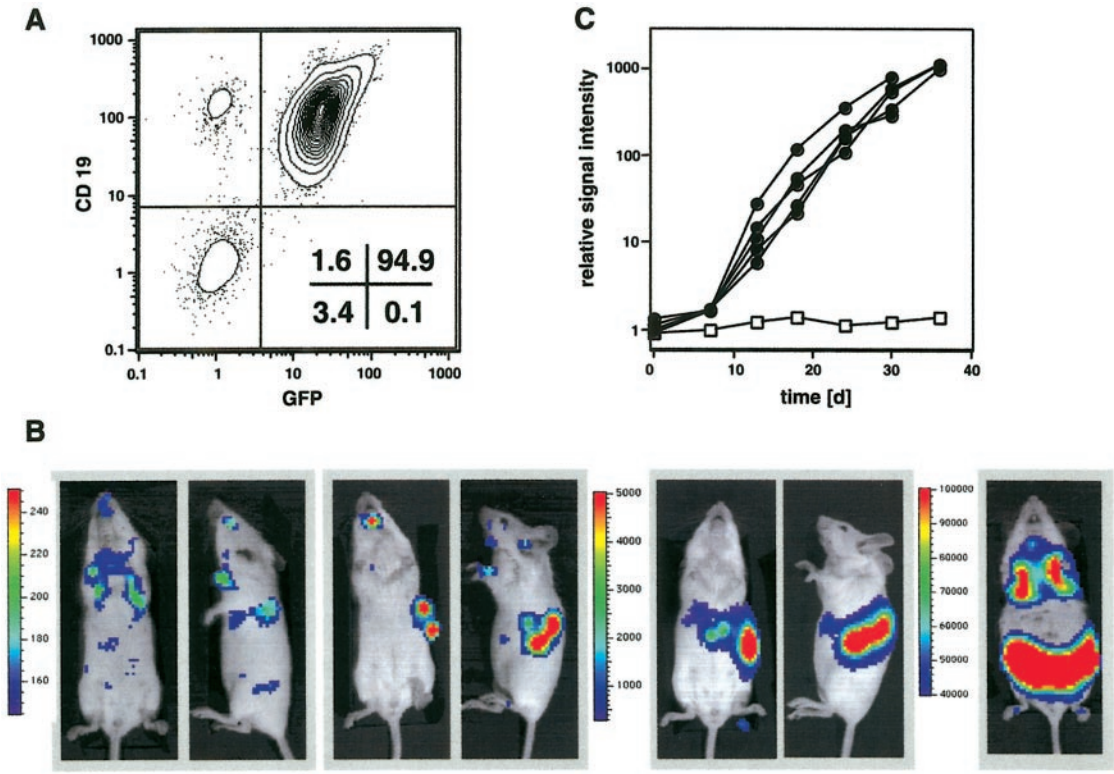

Figure 1. In vivo imaging of BCL_1 lymphoma. (A) BCL_1 lymphoma cells were transduced with the pGC-*gfp/luc* fusion construct, sorted for GFP, and injected intravenously into syngeneic BALB/c mice. GFP^+ cells were passaged 4 times through BALB/c animals and finally through SCID mice to avoid lymphocyte contamination at time of cryoconservation. The final BCL_1-*gfp/luc* cells are $CD19^+$ and show a homogeneous GFP expression. (B) 7×10^3 BCL_1-*gfp/luc* cells were injected intravenously into syngeneic BALB/c mice. Three hours after injection (day 0) a bioluminescent signal (ventral and lateral views) was detectable from the lungs (first 2 images), and after 4 to 5 days tumor engraftment in liver and spleen could be visualized (second 2 images). Tumor growth leading to massive hepato-splenomegaly could be followed over the next 5 weeks (third set of images), and an infiltration of lungs and lymph nodes was observed in final disease stages (5 weeks; final image). The scale to the left of the images describes the color map for the photon count. (C) Quantification of tumor growth by measuring light emission from BALB/c mice after intravenous injection of 2×10^3 BCL_1-*gfp/luc* cells (●, n = 5) compared with a disease-free control animal (□).

animals (n = 5) with cyclophosphamide (2×40 mg/kg intraperitoneally in a 24-hour period) resulted in a substantial reduction in tumor burden (mean, 95.7%; range, 95.0%-96.3%) within the next 4 days. This was followed by a relapse 1 to 2 weeks after treatment and exponential growth of the tumor over the remaining observation time of 5 weeks (Figure 4B). Similarly, tumor response to radiation therapy was assessed by exposing tumor-bearing animals to 8 Gy total body irradiation, followed one day later by a rescue of

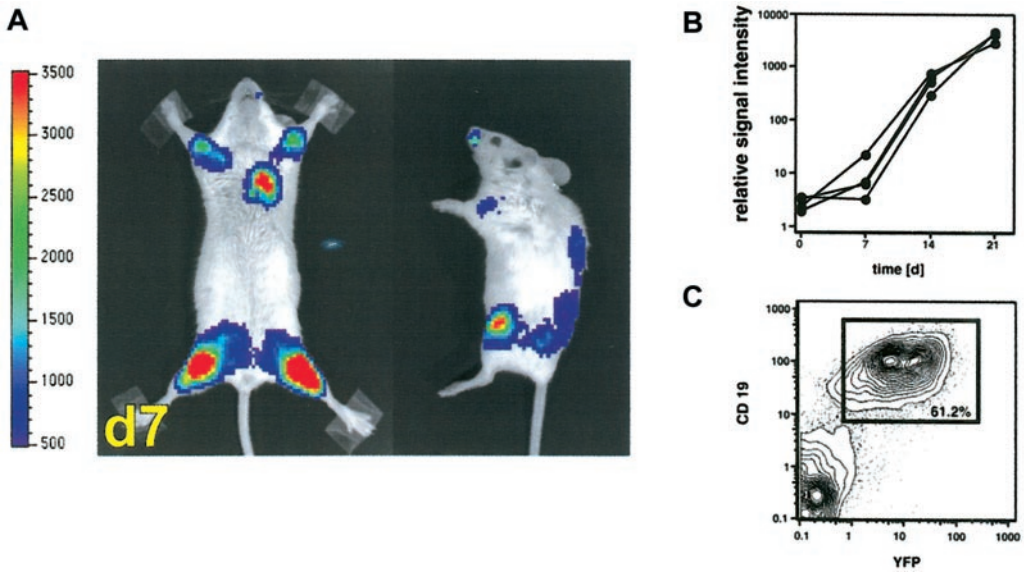

Figure 2. Visualization of leukemic bone marrow infiltration by BLI. (A) Leukemic infiltration of the BM of sublethally irradiated BALB/c mice as revealed by whole body BLI one week after intravenous injection of 2×10^4 A20-*luc/yfp* cells into sublethally irradiated BALB/c mice (4 Gy). The scale to the left of the images describes the color map for the photon count. (B) Tumor expansion as quantified by measuring the photon counts of individual animals (n = 4) emitted at the time points indicated. (C) FACS analysis of BM cells from the femur 21 days after tumor inoculation revealed that 61% of the BM cells were $CD19^+$, YFP^+ tumor cells.

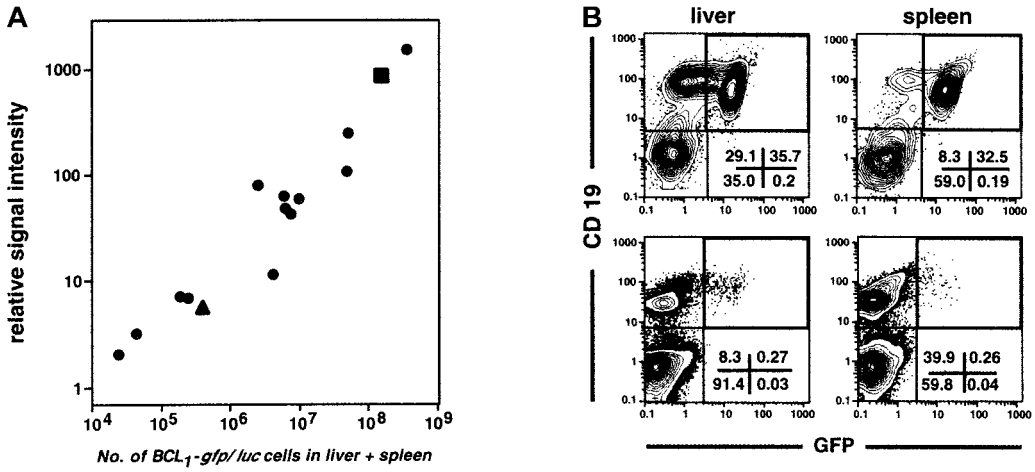

Figure 3. Correlation of bioluminescent signal intensity with tumor burden. (A) Linear correlation (r = 0.989) between bioluminescent signal intensity determined in vivo and tumor burden as determined by FACS analysis of isolated cells from the liver and spleen of tumor-bearing animals (n = 15) 1 to 4 weeks after intravenous injection of 2×10^3 BCL_1-*gfp/luc* cells. (B) FACS plots represent analyses of the hematopoietic cell fraction ($CD45^+$) of liver and spleen from an animal with high (■ in panel A, top row) and one with low tumor load (▲ in panel A, lower row). Numbers represent the percentage of cells within quadrants.

the animal with syngeneic BM cells. As in the control group, tumor engraftment and growth was observed in all animals 14 days after injection (n = 4). There was a significant (mean, 96.2%; range, 94.8%-97.5%) reduction in tumor signal (Figure 4C) 4 days following irradiation. Again, however, all animals relapsed within the next 14 to 21 days. Low-dose irradiation with 2 Gy had no impact on tumor growth (data not shown).

In vivo monitoring of tumor eradication by in vitro–activated and –expanded effector T cells

To explore the impact of an adoptive cellular therapy after allogeneic BMT on disease burden and control of minimal residual disease (MRD), we used ex vivo–activated $CD8^+$ NK-T cells. These cells can be readily expanded from splenocytes or peripheral blood lymphocytes through culture with interferon-γ (IFN-γ), anti-CD3 monoclonal antibodies, and interleukin-2 (IL-2).[19-21] This cytotoxic cell population, termed cytokine induced killer (CIK) cells, shares functional and phenotypic properties of both T and NK cells and recognizes a broad array of both syngeneic and allogeneic tumor targets. In addition, CIK cells have a marked reduction in their ability to cause graft-versus-host disease (GVHD), at least in part due to the production of high levels of IFN-γ.[15] To examine the effects of CIK cells on BCL_1-*gfp/luc* lymphoma growth after allogeneic BMT, we established the lymphoma in recipient BALB/c mice by intravenous injection of 2×10^3 tumor cells and transplanted allogeneic CIK cells 8 days after tumor cell inoculation (24 hours after myeloablative [8 Gy] irradiation). Groups of animals were treated with either 5×10^6 BM cells from C57BL/6 donor animals alone or BM plus 2.5×10^6 C57BL/6 splenocytes or BM plus 2.5×10^6 CIK cells expanded from C57BL/6 mice. Disease burden was assessed by BLI prior to irradiation, 2 days after irradiation, and at weekly intervals thereafter. All animals demonstrated an increase in tumor signal during the first 7 days after tumor inoculation, followed by a reduction of tumor load after irradiation. Using BLI, a quantitative evaluation of tumor burden and response to therapy could be evaluated in individual animals, a unique feature of this imaging strategy. All animals that received only allogeneic BM cells eventually relapsed within 14 to 35 days (Figure 5A) and succumbed to disease several weeks later (Figure 5D). However, time and kinetics of tumor relapse showed a higher variability compared with animals treated with cyclophosphamide or syngeneic BMT (Figure 3), suggesting that alloreactive mechanisms have some influence on tumor relapse kinetics but that these effects are not sufficient for effective tumor control. All animals treated with 2.5×10^6 splenocytes died rapidly from acute GVHD prior to an eventual disease relapse after irradiation (Figure 5B,D). In marked contrast, animals treated with 2.5×10^6 CIK cells maintained control of disease burden after BMT throughout the observation period of 120 days without showing significant signs of GVHD (Figure 5C-D; $P < .0001$).

Unexpectedly, BLI revealed a dramatic change in tumor location at early time points in animals treated with high-dose irradiation and BMT. Following irradiation, a sustained reduction in the splenic signal was clearly demonstrable, accompanied by the emergence of a tumor signal projecting to the central nervous system (CNS) (Figure 5E). This redistribution was observed

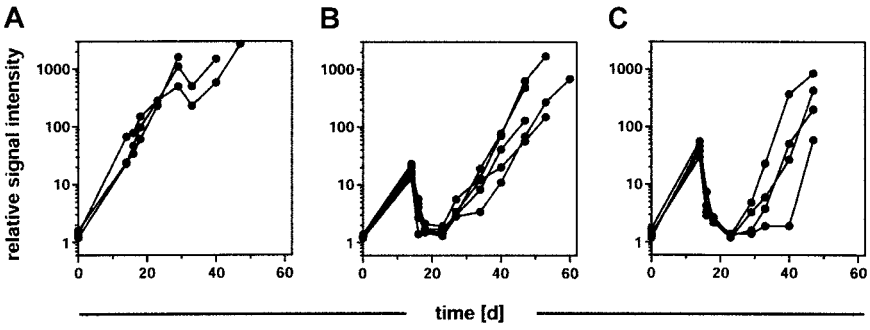

Figure 4. Tumor regression in response to chemotherapy and irradiation therapy. BALB/c mice were engrafted with 2×10^3 BCL_1-*gfp/luc* lymphoma cells, and tumor growth was quantified by BLI 14 days after tumor inoculation. Groups of animals received either (A) no further treatment (n = 3), (B) 2 × 40 mg/kg cyclophosphamide intraperitoneally within 24 hours (n = 5), or (C) total body irradiation with 8 Gy followed 24 hours later by a syngeneic bone marrow transplantation (n = 4). Tumor growth, regression, and relapse were determined by BLI 2 days and 4 days after treatment and in weekly intervals thereafter.

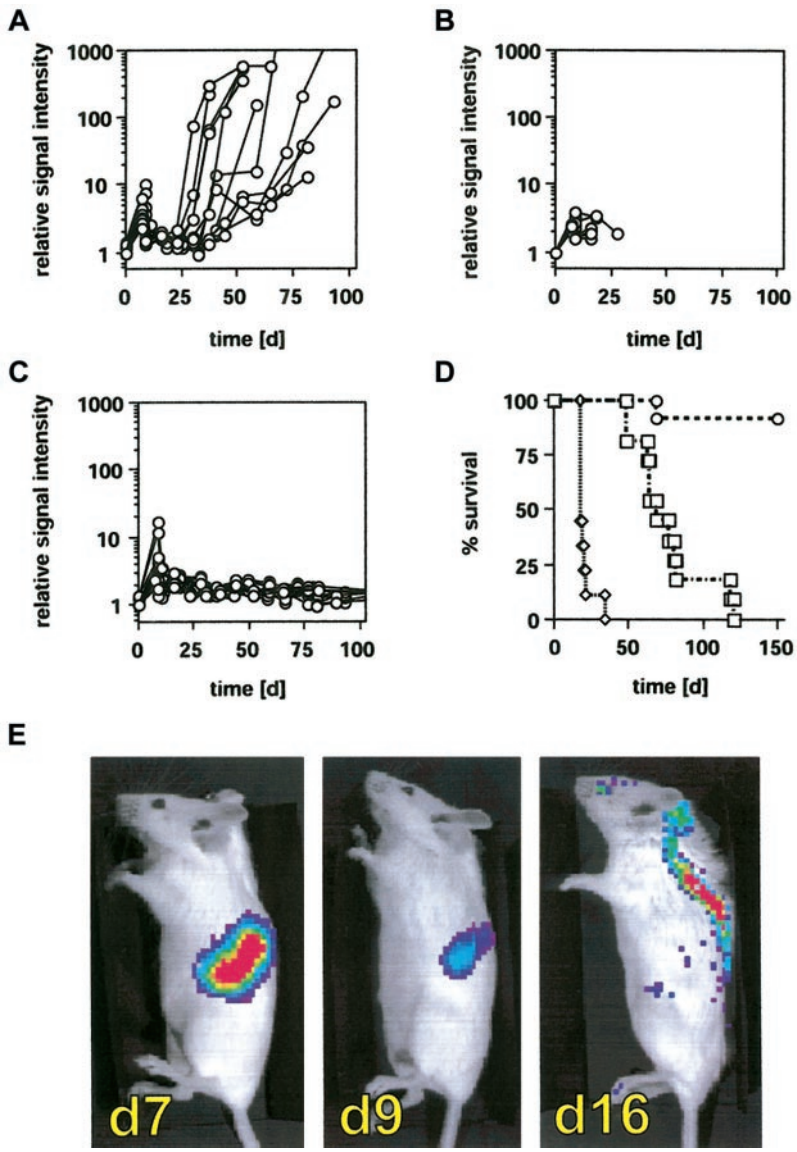

Figure 5. Inhibition of tumor relapse by CIK cells after allogeneic bone marrow transplantation. BALB/c mice (H-2^d) received 2×10^3 BCL_1-*gfp/luc* lymphoma cells intravenously, and tumor engraftment was monitored and quantified by BLI on day 7 as described in "Materials and methods." Following BLI, animals were lethally irradiated (8 Gy) and underwent transplantation within 24 hours with 5×10^6 whole BM cells from C57BL/6 animals (H-2^b). Treatment groups received either (A) BM alone (n = 11), (B) BM + 2.5×10^6 splenocytes (n = 9), or (C) BM + 2.5×10^6 CIK cells (n = 13). Tumor regression following irradiation was determined 2 or 3 days after irradiation, and animals were monitored by BLI for tumor relapse in weekly intervals thereafter (A-C). On the x-axes are days after tumor cell injection. The y-axes are relative light emission from individual animals over a 5-minute integration time. (D) Survival of animals from treatment groups A (□), B (△), and C (○); on the x-axis are days after tumor cell injection. On the y-axis is the proportion of recipients surviving. ($P < .0001$ between all treatment groups.) (E) Tumor distribution pattern of one representative animal prior to irradiation (day 7), 2 days after irradiation (day 9), and 9 days after irradiation (day 16).

beginning 1 week after irradiation and was uniformly seen in animals surviving beyond that time point irrespective of the treatment regimen (BMT ± CIK cells). The signal from these sites did not increase over time, suggesting that no significant tumor cell expansion occurred and no neurologic deficit was noted in these animals. In the A20-*yfp/luc* tumor model, however, animals experienced an irradiation dose-dependent meningeal tumor infiltration and suffered hind limb paralysis 15 to 25 days following BMT caused by tumor compression of the spinal cord. While low-dose irradiation with 2 Gy did not lead to paralysis (n = 7), paralysis was observed in 66% of animals that received 4 Gy total body irradiation (8 of 12) and in all animals treated with 6 Gy (n = 7) or 8 Gy and rescued by a syngeneic or allogeneic BMT (n > 30). BLI performed ex vivo on freshly isolated spinal cords as well as histopathological evaluation revealed meningeal disease with tumor studding of the spinal cord (data not shown).

Tracking of effector T cells in tumor-bearing mice

Since lymphoma cells and CIK cells migrate to the same organs following intravenous injection, we examined effector cell migration to an ectopic tumor site in a syngeneic tumor model. For this purpose, BALB/c splenocytes were transduced with the *gfp/luc* retrovirus and expanded under CIK culture conditions. 5×10^6 CIK cells (25% GFP^+) were injected intravenously into syngeneic BALB/c animals bearing macroscopic tumors generated by subcutaneous injection of 1×10^7 A20-lymphoma cells 10 days prior to treatment (Figure 6). The injection site was shaved to allow for external tumor visualization. Thirty minutes after intravenous injection, Luc^+ CIK cells could be detected by BLI in the lungs of the animals. This was followed by a more general distribution of the cells to other sites within the body, such as liver and spleen, within the next 16 hours. By 72 hours, a clearly defined population of labeled effector cells infiltrated the subcutaneous tumor on the flank of the animal. Luc-expressing CIK cells remained detectable by BLI at the tumor site for an additional period of 9 days, over which time the tumor mass completely regressed. Of 6 animals treated with expanded CIK cells (in 2 separate experiments), 5 did not show any signs of tumor relapse throughout the observation period of 6 months. In contrast, all untreated animals developed large tumor masses and were humanely killed within 12 weeks due to severe progressive disease (n = 6). These studies demonstrate

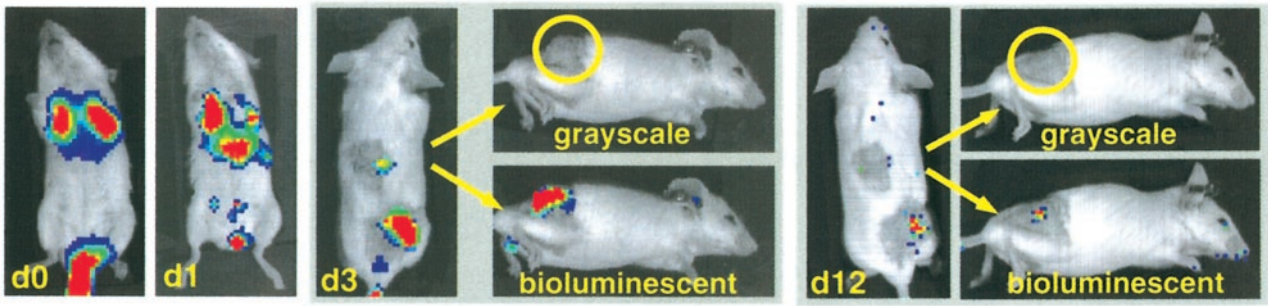

Figure 6. Trafficking of CIK cells. BALB/c splenocytes were retrovirally transduced with the pGC-*gfp/luc* vector, FACS sorted, and expanded under CIK culture conditions as described in "Material and methods." Transduced CIK cells were injected intravenously into syngeneic animals bearing a macroscopically visible A20-lymphoma subcutaneously (n = 6 in 2 separate experiments). Shown in the figure is the repetitive imaging of one representative animal. Day 0: early localization of CIK cells to the lungs; day 1: distribution to other sites, including liver and spleen; day 3: preferential infiltration of subcutaneous tumor site (shaved area, lower right quadrant, and shaved control area in the middle of the back of the animal); day 12: regression of tumor and minimal signal from remaining CIK cells. For days 3 and 12, tangential photographs (grayscale) are shown for a better tumor localization and the bioluminescent overlay (bioluminescence) for CIK cell localization.

that BLI can be readily used to assess the antitumor activity of expanded $CD8^+$ NK-T cells in vivo in both syngeneic and allogeneic animal models.

Discussion

Animal models of leukemia and lymphoma are critically important for both the study of the basic biology of these malignancies as well as for the development of improved therapeutic interventions. The examination of complex biological processes such as tumor growth, metastasis, and response to therapy requires animal models capable of detecting small numbers of cells, noninvasively and quantitatively. We previously described a new bioluminescence-based imaging technology allowing the noninvasive detection of human tumor cells in living severe combined immunodeficient (SCID) animals with high sensitivity.[8,11] In these initial experiments, the human cervical carcinoma cell line HeLa-*luc* was engrafted into SCID animals for proof of principle. However, neither tumor cell nor effector cell trafficking could reliably be evaluated in these xenogenic systems. Here, we describe 2 tumor models allowing for the in vivo examination of leukemia and lymphoma cell trafficking and proliferation in real time. For this purpose, we used dual function reporter genes to link the powerful in vivo analyses via bioluminescence imaging (BLI) to the cell discriminating ex vivo assays that employ flow cytometry.[22] The fluorescent function of the gene fusion allows for the isolation and recovery of transduced cells either before or after the cell distribution patterns are revealed in living animals using the bioluminescent component of the dual function reporter gene.[23] The results presented in this report demonstrate the remarkable sensitivity of bioluminescence-based imaging strategies and the ability to quantitatively measure tumor burden over the entire spectrum of disease from minimal to massive tumor burden in individual animals.

This approach has several advantages over conventional tumor models: the sensitivity of cell detection in vivo is surprisingly high and exceeds even the sensitivity of detection by flow cytometry ex vivo. As few as 7×10^3 cells are detectable in the lungs early after injection, 2-2.5 $\times 10^4$ cells within liver or spleen, and as few as 1×10^4 tumor cells within the BM of a femur give rise to a sufficient signal to be detected externally. In other experiments using cells with even higher luciferase expression, as few as 100 cells can be reliably detected in the peritoneal cavity of living animals. Since cells are detectable even from deep within tissues, tumor cell trafficking, engraftment in different organs, and metastasis could be visualized without perturbing intact organ systems. Given that the amount of light emitted from tumor-bearing animals can be quantified externally at serial time points, tumor growth kinetics can be evaluated noninvasively. Using the fluorescent component of the dual function reporter genes for the re-isolation of lymphoma cells from tumor-bearing mice reveals that the signal intensity detected externally correlates highly with tumor load ($r = 0.989$). This high correlation allows for extrapolation of the in vivo tumor cell doubling time and verifies that the signal intensity reflects tumor load reliably to allow for the quantitative evaluation of the effects of cytostatic and cytotoxic therapies. As examples, response to chemotherapy and radiation therapy were studied, confirming that even minimal residual disease is detectable and that location, timing, and kinetics of tumor relapse could be determined. Using this technology, it is now possible to study early events in tumor development long before any clinical signs of disease are evident as well as the efficiency of therapeutic interventions in minimal disease stages. These new tools will improve our understanding of tumor biology and tumor immunology and facilitate drug discovery and evaluation.

Thusfar, we have used tumor cell lines to examine the effects of chemotherapy, radiation, and immunotherapy. The inclusion of bioluminescent reporter genes into inducible transgenes for the targeted overexpression of oncogenes and/or tumor suppressor gene mutant systems could be used in "spontaneous" models of malignancy to facilitate the examination of early molecular events in carcinogenesis.[24] Recently, Vooijs et al reported the successful integration of bioluminescent reporter genes in such a model system using retinoblastoma (*Rb*) mutant animals for the study of pituitary gland tumor development.[25] Similar systems for the study of "spontaneous" models of hematopoietic malignancy are currently under development. Given the good sensitivity of cell detection from within the bone marrow, such approaches will greatly facilitate the examination of early molecular and cellular events in leukemia development and hematopoietic stem cell biology. The transduction of nonmalignant hematopoietic stem cells with optical reporter genes will furthermore greatly facilitate the examination of trafficking and expansion of precursor cells after BMT.

We have used these bioluminescent tumor models to assess the antilymphoma effect of adoptive cellular immunotherapy after allogeneic BMT. To do this, we infused ex vivo–expanded $CD8^+$ T cells, which share functional and phenotypic properties with NK cells (CIK cells). CIK cells are capable of protecting animals from an otherwise lethal challenge of BCL_1 tumor cells, using either

syngeneic or allogeneic effector cells.[15] As described previously, CIK cells cause much less GVHD than splenocytes when transplanted across major histocompatibility barriers, in part due to the production of IFN-γ, since CIK cells derived from animals incapable of producing this cytokine result in rapid lethal GVHD.[15] Here, we show that CIK cells are capable of inhibiting BCL_1-*gfp/luc* relapse as assessed serially by BLI without causing GVHD. The infusion of freshly isolated splenocytes resulted in acute GVHD and rapid animal death even before reaching the time of relapse of BM control groups. The effects of CIK cells appeared to occur rapidly following infusion and prevented the early growth of BCL_1-*gfp/luc*. The strategy of using CIK cells that have a rapid onset of action due to prior in vitro activation may be particularly valuable in disease conditions where early relapse is a high risk. Following nonmyeloablative conditioning regimens, CIK treatment may control disease burden prior to the delayed onset of GVL effects generated by immune cells derived from the transplanted BM. Such strategies are currently under investigation. In our tumor models, BLI revealed an infiltration of the CNS by lymphoma cells following high-dose whole body irradiation and BMT. This unexpected finding demonstrates that unique trafficking patterns can result following therapeutic interventions that can be revealed only by sensitive in vivo imaging techniques.[26] Since the CNS is a frequent sanctuary site in hematological malignancies, this finding was of particular interest. CNS relapse has been observed following transplantation, even in clinical situations where this may not be predicted (eg, in patients with multiple myeloma). Therefore, evaluation of the impact of different preparative regimens with respect to dose of irradiation and impact of chemotherapy on CNS infiltration with malignant cells can be directly studied with BLI and could have important ramifications in clinical bone marrow transplantation.

In a second tumor therapy model we directly evaluated the in vivo fate of CIK cells following retroviral marking with GFP and Luc. Labeled CIK cells were initially visualized over the lungs following intravenous injection. Within 24 hours they migrated to extra-pulmonic sites, and by 3 days the infiltration of a subcutaneous lymphoma could be directly visualized. The effector cells persisted at this location for at least 9 days, resulting in tumor eradication. These results are in agreement with our in vitro observations that cell contact is necessary for antitumor cytotoxicity.[21] These studies further demonstrate that the biologic effects of CIK cells occur rapidly and that the cells persist in vivo for approximately 2 weeks. It should be noted that these studies were performed without the administration of additional cytokines such as IL-2, which may be a unique advantage of CIK cells over other preparations of NK-like cells such as lymphokine-activated killer (LAK) cells.[19] For CIK cells, we have previously demonstrated the critical role of perforin for their tumor eradication in vivo, whereas Fas-L appears to be less important.[27] The future evaluation of additional effector and target recognition molecules and their differential use by different lymphocyte populations may provide novel insights into the role of these gene products in lymphocyte biology and tumor immune surveillance.

The use of BLI for the evaluation of adoptively transferred cells allows the study of their fate in vivo throughout the entire course of immunotherapy. Following intravenous administration, their migration through lungs and internal organs like liver, spleen, and lymph nodes is visualized as well as their arrival at tumor sites and disease eradication. The goal of ongoing studies is the evaluation of key molecular mechanisms required for completion of various steps in this process. Cellular migration in and out of organs through endothelial barriers and into tissues is well orchestrated by adhesion molecules and chemokines.[28] The use of knock-out animals lacking these molecules as recipients or cell donors will reveal some of the main mechanisms involved in this process. In our studies, only a subset of injected CIK cells are found at the tumor site. The re-isolation and characterization of the cells infiltrating the tumor tissue and their comparison to cells migrating to other sites is another approach currently under investigation for the identification of molecules involved. A limitation of this strategy is the relatively low transduction efficiency of retroviral vectors for primary lymphocyte populations and the risk of gene silencing.[29,30] Transduction efficiencies of 10%-30% are adequate to image the transduced lymphocyte populations due to the remarkable sensitivity of BLI. However, higher levels of gene marking will significantly facilitate cell recovery from the animals. Other approaches, such as the use of lentiviral vector systems and the generation of transgenic animals with constitutive or inducible expression of bioluminescent reporter genes will be important in overcoming these limitations. One concern is the possibility that the reporter genes could be immunogenic, as previously described for GFP.[31,32] In our experiments, however, we could not detect any enhanced immune recognition of BCL_1-*gfp/luc* cells, and the observation period for transduced CIK cells might have been too short for an immune response to occur.

In this study we further refined BLI as a powerful tool for the study of neoplastic disease by using the dual function reporter genes. This noninvasive, highly sensitive, and quantitative approach is ideally suited for evaluating complex biologic processes in vivo such as lymphocyte trafficking and tumor eradication. These studies allowed, for the first time, real-time visualization of GVL activity. Using BLI, all of the steps required for effective adoptive immunotherapy following intravenous injection of cells including migration through the lungs, spleen, and infiltration of tumor tissues can be visualized and studied. Further evaluation of the cells that effectively localize to tumor tissue is a major advantage of this approach and the goal of future studies.

Acknowledgments

We thank Dr Petra Hoffmann for helpful discussions during the course of this project and critical review of the manuscript. We thank Ruby Wong for statistical analysis and Jeanette Baker for her excellent help with the experiments.

References

1. Thomas ED, Blume KG, Forman SJ. Hematopoietic cell transplantation. 2nd ed. Malden, MA: Blackwell Science; 1999.
2. Kolb HJ, Mittermuller J, Clemm CH, et al. Donor leukocyte transfusions for treatment of recurrent chronic myelogenous leukemia in marrow transplant patients. Blood. 1990;76:2462-2465.
3. Weiden PL, Sullivan KM, Flournoy N, Storb R, Thomas ED. Antileukemic effect of chronic graft versus host disease: contribution of improved survival after allogeneic marrow transplantation. N Engl J Med. 1981;304:1529-1533.
4. Lyons AB. Analysing cell division in vivo and in vitro using flow cytometric measurement of CFSE dye dilution. J Immunol Methods. 2000;243:147-154.
5. Okabe M, Ikawa M, Kominami K, Nakanishi T, Nishimune Y. "Green mice" as a source of ubiquitous green cells. FEBS Lett. 1997;407:313-319.
6. Wilson T, Hastings JW. Bioluminescence. Annu Rev Cell Dev Biol. 1998;14:197-230.

7. Hastings JW. Chemistries and colors of bioluminescent reactions: a review. Gene. 1996;173:5-11.
8. Sweeney TJ, Mailander V, Tucker AA, et al. Visualizing the kinetics of tumor-cell clearance in living animals. Proc Natl Acad Sci U S A. 1999;96:12044-12049.
9. Contag CH, Contag PR, Mullins JI, Spilman SD, Stevenson DK, Benaron DA. Photonic detection of bacterial pathogens in living hosts. Mol Microbiol. 1995;18:593-603.
10. Contag PR, Olomu IN, Stevenson DK, Contag CH. Bioluminescent indicators in living mammals. Nat Med. 1998;4:245-247.
11. Edinger M, Sweeney TJ, Tucker AA, Olomu AB, Negrin RS, Contag CH. Noninvasive assessment of tumor cell proliferation in animal models. Neoplasia. 1999;1:303-310.
12. Costa GL, Benson JM, Seroogy CM, Achacoso P, Fathman CG, Nolan GP. Targeting rare populations of murine antigen-specific T lymphocytes by retroviral transduction for potential application in gene therapy for autoimmune disease. J Immunol. 2000;164:3581-3590.
13. Robbins PB, Yu XJ, Skelton DM, et al. Increased probability of expression from modified retroviral vectors in embryonal stem cells and embryonal carcinoma cells. J Virol. 1997;71:9466-9474.
14. Eberl G, MacDonald HR. Rapid death and regeneration of NKT cells in anti-CD3epsilon- or IL-12-treated mice: a major role for bone marrow in NKT cell homeostasis. Immunity. 1998;9:345-353.
15. Baker J, Verneris MR, Ito M, Shizuru JA, Negrin RS. Expansion of cytolytic CD8(+) natural killer T cells with limited capacity for graft-versus-host disease induction due to interferon gamma production. Blood. 2001;97:2923-2931.
16. Rice B, Cable M, Nelson M. In vivo imaging of light-emitting probes. J Biomed Opt. 2001;6:432-440.
17. Warnke RA, Slavin S, Coffman RL, et al. The pathology and homing of a transplantable murine B cell leukemia (BCL1). J Immunol. 1979;123:1181-1188.
18. Strober S, Gronowicz ES, Knapp MR, et al. Immunobiology of a spontaneous murine B cell leukemia (Bcl-1). Immunol Rev. 1979;48:169-195.
19. Lu PH, Negrin RS. A novel population of expanded human CD3+CD56+ cells derived from T cells with potent in vivo antitumor activity in mice with severe combined immunodeficiency. J Immunol. 1994;153:1687-1696.
20. Schmidt-Wolf IG, Negrin RS, Kiem HP, Blume KG, Weissman IL. Use of a SCID mouse/human lymphoma model to evaluate cytokine-induced killer cells with potent antitumor cell activity. J Exp Med. 1991;174:139-149.
21. Schmidt-Wolf IG, Lefterova P, Mehta BA, et al. Phenotypic characterization and identification of effector cells involved in tumor cell recognition of cytokine-induced killer cells. Exp Hematol. 1993;21:1673-1679.
22. Day RN, Kawecki M, Berry D. Dual-function reporter protein for analysis of gene expression in living cells. Biotechniques. 1998;25:848-850,852-844, 856.
23. Costa GL, Sandora MR, Nakajima A, et al. Adoptive immunotherapy of experimental autoimmune encephalomyelitis via T cell delivery of the IL-12 p40 subunit. J Immunol. 2001;167:2379-2387.
24. Resor L, Bowen TJ, Wynshaw-Boris A. Unraveling human cancer in the mouse: recent refinements to modeling and analysis. Hum Mol Genet. 2001;10:669-675.
25. Vooijs M, Jonkers J, Lyons S, Berns A. Noninvasive imaging of spontaneous retinoblastoma pathway-dependent tumors in mice. Cancer Res. 2002;62:1862-1867.
26. Merrill JE, Murphy SP. Inflammatory events at the blood brain barrier: regulation of adhesion molecules, cytokines, and chemokines by reactive nitrogen and oxygen species. Brain Behav Immun. 1997;11:245-263.
27. Verneris MR, Ito M, Baker J, Arshi A, Negrin RS, Shizuru JA. Engineering hematopoietic grafts: purified allogeneic hematopoietic stem cells plus expanded CD8+ NK-T cells in the treatment of lymphoma. Biol Blood Marrow Transplant. 2001;7:532-542.
28. Butcher EC, Williams M, Youngman K, Rott L, Briskin M. Lymphocyte trafficking and regional immunity. Adv Immunol. 1999;72:209-253.
29. Klug CA, Cheshier S, Weissman IL. Inactivation of a GFP retrovirus occurs at multiple levels in long-term repopulating stem cells and their differentiated progeny. Blood. 2000;96:894-901.
30. Halene S, Wang L, Cooper RM, Bockstoce DC, Robbins PB, Kohn DB. Improved expression in hematopoietic and lymphoid cells in mice after transplantation of bone marrow transduced with a modified retroviral vector. Blood. 1999;94:3349-3357.
31. Stripecke R, Carmen Villacres M, Skelton D, Satake N, Halene S, Kohn D. Immune response to green fluorescent protein: implications for gene therapy. Gene Ther. 1999;6:1305-1312.
32. Gambotto A, Dworacki G, Cicinnati V, et al. Immunogenicity of enhanced green fluorescent protein (EGFP) in BALB/c mice: identification of an H2-Kd-restricted CTL epitope. Gene Ther. 2000;7:2036-2040.